

Research Article

# Dual-Domain Temporal–Spatial Denoising Approach for Autism Spectrum Disorder EEG Signals Based on Stationary Wavelet Transform and SPHARA

Cut Siti Azola Syiva <sup>1</sup>, Melinda Melinda <sup>1\*</sup>, Syahrial Syahrial <sup>1</sup>, Imam Fathur Rahman <sup>1</sup>, Souvik Das <sup>2</sup>, and M. Ary Heryanto <sup>3</sup>

<sup>1</sup> Department of Electrical and Computer Engineering, Faculty of Engineering, Syiah Kuala University, Banda Aceh 23111, Indonesia;


e-mail : csitia@mhs.usk.ac.id; melinda@usk.ac.id; syahrial@usk.ac.id; imamfth@mhs.usk.ac.id

<sup>2</sup> Department of Industrial Design, National Institute of Technology Rourkela, Rourkela 769008, India;

e-mail : rndas9@gmail.com

<sup>3</sup> Faculty of Engineering, Universitas Dian Nuswantoro, Semarang, Central Java 50131, Indonesia;

e-mail : m.aryheryanto@dsn.dinus.ac.id

\* Corresponding Author : Melinda Melinda 

**Abstract:** Electroencephalography (EEG) signals are highly susceptible to noise and artifacts, which can degrade analysis accuracy, particularly in Autism Spectrum Disorder (ASD) studies. Therefore, effective preprocessing is required to improve signal quality prior to further analysis. This study proposes an integrated EEG preprocessing pipeline that combines a Finite Impulse Response (FIR) band-pass filter (0.5–70 Hz) with notch filtering and detrending, followed by temporal denoising using the Stationary Wavelet Transform (SWT) with the Daubechies 4 mother wavelet and spatial filtering based on SPHARA. This dual-domain approach is designed to address both temporal and spatial noise in multichannel EEG signals. Experimental results demonstrate that the proposed FIR combined with SWT and SPHARA pipeline consistently outperforms single-domain preprocessing methods, achieving a maximum Signal-to-Noise Ratio (SNR) of 31.93 dB. The proposed method also produces the lowest Mean Absolute Error (MAE) (16.81  $\mu$ V) and Standard Deviation (SD) (0.75  $\mu$ V), indicating high signal stability with minimal amplitude distortion. Root Mean Square Error (RMSE) values remain stable within the range of 29.5–592.3  $\mu$ V, with a minimum RMSE of 29.5  $\mu$ V, demonstrating effective noise suppression while preserving signal energy. These results confirm that integrating temporal and spatial preprocessing significantly improves EEG signal quality and supports more reliable EEG analysis for ASD-related studies.

**Keywords:** Autism Spectrum Disorder; Biomedical Signal Processing; EEG Preprocessing; Electroencephalography; Signal Denoising; Multichannel EEG; Stationary Wavelet Transform; SPHARA.

Received: March, 17<sup>th</sup> 2026

Revised: April, 14<sup>th</sup> 2026

Accepted: April, 15<sup>th</sup> 2026

Published: April, 23<sup>rd</sup> 2026



**Copyright:** © 2026 by the authors. Submitted for possible open access publication under the terms and conditions of the Creative Commons Attribution (CC BY) licenses (<https://creativecommons.org/licenses/by/4.0/>)

## 1. Introduction

Autism Spectrum Disorder (ASD) is a multidimensional neurodevelopmental disorder. ASD is generally characterized by difficulties in communication, social interaction, and repetitive behaviors. Based on data reported by the World Health Organization (WHO), the prevalence of individuals with ASD continues to increase globally, with an estimated 1 in 100 children diagnosed with ASD [1]. Early detection of ASD is therefore very important to enable timely interventions and improve the quality of life of individuals with ASD. However, the diagnosis of ASD still relies on a combination of the Autism Diagnostic Observation Schedule (ADOS) and the Autism Diagnostic Interview–Revised (ADI-R), which require intensive training and a considerable amount of time. Consequently, these diagnostic procedures are typically applied only in specialized clinics with limited capacity [2].

Electroencephalography (EEG) offers a promising alternative because it can record the electrical activity of the brain in real time, in a non-invasive manner, and at a relatively affordable cost. Resting-state studies show that individuals with ASD exhibit unusual patterns of neural synchronization and functional connectivity, reflecting an imbalance in the integration of internal and external information across various brain networks [3]. Other studies have reported increased power in the beta and gamma frequency bands, as well as changes in resting-state connectivity patterns, which distinguish individuals with ASD from neurotypical individuals [4]. These findings reinforce the potential of EEG as a neurophysiological biomarker for distinguishing ASD and neurotypical conditions more objectively than behavioral observations alone. In order to optimize the extraction of relevant neural information, an effective preprocessing design is required to improve signal quality before the feature extraction and classification stages.

EEG signals generally have a low signal-to-noise ratio (SNR) and are highly susceptible to both temporal and spatial interference. Temporal noise includes baseline shifts, eye blinks and eye movements, muscle activity, and electrical interference that may alter the amplitude, phase, and latency of signal components, thereby reducing the reliability of feature estimation [5]. Spatial noise arises due to volume conduction and spatial leakage, where activity from the same neural source spreads across multiple electrodes, emphasizing global low-spatial-frequency patterns and masking local information that is important for topographic and connectivity analysis [6]. This challenge becomes even greater in low-density EEG configurations, where the limited number of electrodes makes local information more easily dominated by global patterns. In dry EEG systems, the absence of conductive gel may further increase impedance instability and motion artifacts [7], whereas in wet EEG systems, temporal and spatial disturbances still remain major issues that must be addressed systematically.

To reduce the impact of noise on EEG signals, several studies have proposed the integration of temporal and spatial artifact removal techniques. One example is the use of Independent Component Analysis (ICA)-based Fingerprint and Automatic Removal of Cardiac Interference (ARCI) combined with SPHERical HARMonic Analysis (SPHARA) and its improved variant incorporating an amplitude-zeroing step (AP0) for high-density 64-channel dry EEG recordings [7], [8]. In such frameworks, ICA is used to separate signal sources so that components corresponding to artifacts can be identified and suppressed before signal reconstruction. However, since this approach was primarily developed and evaluated for high-density EEG configurations, its application to low-density EEG systems such as 16-channel recordings generally requires methodological adjustments to maintain practicality and stability.

On the low-density side, a 16-channel resting-state EEG dataset involving individuals with ASD and neurotypical controls has previously been used in feature-based classification studies comparing Empirical Wavelet Transform (EWT) and Empirical Mode Decomposition (EMD) with EEGNet and ShallowFBCSPNet architectures [9]. In that study, explicit signal preprocessing prior to the decomposition stage was still limited mainly to band-pass filtering, while EWT and EMD were utilized as feature extraction techniques for the classification stage. Strategies specifically designed to mitigate high-amplitude transient temporal artifacts as well as inter-channel spatial leakage have not been the main focus. Therefore, there remains an opportunity to develop a preprocessing framework that explicitly addresses both temporal and spatial noise within the same 16-channel EEG dataset.

Considering these limitations, this study designs an integrated and automated preprocessing pipeline for 16-channel EEG signals to improve signal quality comprehensively. The proposed preprocessing framework applies a Finite Impulse Response (FIR) band-pass filter (0.5–70 Hz) with linear phase, a 50 Hz notch filter, and constant detrending as the initial stage to suppress low-frequency drift, power-line interference, and non-physiological high-frequency components associated with muscle activity and acquisition system noise [5], [10]. Further temporal denoising is performed using the Stationary Wavelet Transform (SWT) to reduce transient high-amplitude artifacts and unstable medium- to high-frequency components, while spatial filtering is applied using SPHARA as a harmonic-based spatial filtering approach that follows the geometry of the 16-channel EEG electrode configuration.

To the best of our knowledge, limited studies have investigated the integration of temporal wavelet-based denoising and spatial harmonic filtering specifically for low-density 16-channel EEG signals in ASD resting-state analysis. Therefore, this study aims to evaluate an

integrated preprocessing pipeline that simultaneously addresses temporal and spatial noise in EEG signals.

The objective of this study is to evaluate the performance of the proposed preprocessing pipeline through four configurations: FIR, FIR combined with SWT, FIR combined with SPHARA, and the integrated FIR–SWT–SPHARA approach. Each configuration is evaluated using SNR, Root Mean Square Error (RMSE), Mean Absolute Error (MAE), and Standard Deviation (SD). Although the dataset includes both ASD and neurotypical subjects, this study focuses specifically on the ASD group to evaluate the effectiveness of the proposed preprocessing pipeline on EEG signals associated with ASD.

Through this evaluation, the study aims to identify a standardized and effective preprocessing pipeline suitable for low-density 16-channel EEG configurations for ASD resting-state EEG data. The main contributions of this study are summarized as follows:

- The development of an integrated preprocessing pipeline specifically designed for low-density 16-channel EEG signals in ASD resting-state analysis.
- The integration of temporal denoising using SWT and spatial filtering using SPHARA to simultaneously address temporal and spatial noise in EEG signals.
- A comparative evaluation of four preprocessing configurations: FIR, FIR combined with SWT, FIR combined with SPHARA, and FIR combined with SWT and SPHARA.
- A quantitative performance assessment using SNR, RMSE, MAE, and SD to analyze improvements in EEG signal quality.

The remainder of this paper is organized as follows. Section 2 presents the theoretical background and related works on EEG preprocessing techniques. Section 3 describes the proposed EEG preprocessing methodology, including dataset description and preprocessing pipeline design. Section 4 presents the experimental results and discussion. Finally, Section 5 concludes the paper and outlines potential directions for future research.

## 2. Literature Review

### 2.1. Autism Spectrum Disorder

Autism Spectrum Disorder (ASD) is a neurodevelopmental condition characterized by persistent difficulties in social communication and interaction, accompanied by restricted and repetitive behavioral patterns. The severity of symptoms varies widely among individuals, forming a spectrum that ranges from mild to severe functional impairment. In modern clinical classification, previously distinct conditions such as classical autism, Asperger syndrome, and Pervasive Developmental Disorder–Not Otherwise Specified (PDD-NOS) are now grouped under ASD to emphasize the continuum of symptoms within a single spectrum [11].

Early indicators of ASD may include delayed language development, reduced eye contact, and limited responses to social cues. Because early detection and intervention have been shown to significantly improve developmental outcomes, the development of objective and reliable detection approaches has become an important research focus in recent years [12]. EEG has been widely utilized to investigate neural activity patterns associated with ASD. It provides non-invasive measurements of brain electrical activity with high temporal resolution, allowing researchers to analyze neural oscillations and functional connectivity differences between individuals with ASD and neurotypical populations. Several studies have reported atypical neural synchronization and altered spectral characteristics in ASD, suggesting that EEG signals may provide valuable biomarkers for understanding neural mechanisms and supporting the development of objective ASD analysis methods [13].

### 2.2. EEG Noise Characteristics

EEG is widely used to investigate neural activity because it provides non-invasive measurements of brain electrical signals with high temporal resolution. However, EEG recordings are highly susceptible to various types of noise and artifacts that may distort the underlying neural information. Previous studies have emphasized that EEG recordings are sensitive to both physiological and non-physiological artifacts, which may significantly distort neural information and reduce the reliability of downstream signal analysis if not properly handled during preprocessing [14].

### 2.2.1. Temporal Noise

Temporal noise refers to disturbances that vary over time and affect the amplitude, morphology, and slope of EEG waveforms. These disturbances commonly originate from instability at the electrode–skin interface, electrode displacement, cable movement, and variations in contact impedance during recording [7]. Physiological artifacts such as eye blinks and eye movements typically introduce low-frequency disturbances, whereas muscle activity generates higher-frequency components that may overlap with beta and gamma bands. These transient artifacts may significantly degrade the reliability of EEG signal analysis if not properly addressed during preprocessing [15].

### 2.2.2. Spatial Noise

In addition to temporal disturbances, EEG recordings may also contain spatial noise that appears as abnormal amplitude distributions across channels. Physiological brain activity recorded through volume conduction typically produces spatially smooth patterns across the scalp. In contrast, spatial noise introduces irregular spatial variations that distort topographic signal distributions [16], [17]. Such disturbances may arise from unstable electrode contact, high impedance, cable movement, or localized muscle activity affecting specific channels. Therefore, effective preprocessing techniques are required to suppress spatial disturbances while preserving physiologically meaningful neural patterns.

## 2.3. Study Gap and Motivation

Several studies have investigated artifact removal techniques in EEG preprocessing. ICA and its variants have been widely applied to separate neural signals from artifacts, particularly in high-density EEG systems. In such settings, ICA-based frameworks are often combined with spatial filtering techniques such as SPHARA to enhance artifact suppression and signal reconstruction [7], [8]. However, these approaches are primarily designed for high-density configurations and may not be directly applicable to low-density EEG systems due to the limited number of available channels.

In low-density EEG studies, preprocessing pipelines are often simplified. For example, previous research using 16-channel resting-state EEG data for ASD classification mainly relied on band-pass filtering prior to feature extraction methods such as EWT and EMD [9]. Although these approaches achieved promising classification performance, the preprocessing stage did not explicitly address transient temporal artifacts or spatial leakage across channels. As a result, noise components may still persist and affect signal quality.

These observations highlight a key limitation in existing studies: temporal and spatial noise are often treated independently, particularly in low-density EEG configurations. While temporal denoising methods aim to suppress non-stationary artifacts, and spatial filtering techniques focus on inter-channel noise, their integration remains limited. Consequently, there is a lack of preprocessing frameworks that simultaneously address both temporal disturbances and spatial noise in low-density EEG data.

From a methodological perspective, commonly used approaches such as ICA, EMD, and DWT exhibit inherent limitations in this context. ICA relies on multichannel source separation and generally performs better in high-density systems, making it less suitable for low-density EEG. Meanwhile, EMD- and DWT-based approaches primarily focus on temporal decomposition and do not explicitly model spatial relationships across channels. These limitations motivate the need for a more integrated preprocessing strategy.

In this study, SWT and SPHARA are selected based on their complementary characteristics and suitability for low-density EEG configurations. Compared to DWT, SWT provides translation-invariant decomposition, which preserves signal alignment and reduces distortion in non-stationary signals. In contrast to EMD, SWT offers more stable and consistent decomposition. On the spatial side, SPHARA explicitly incorporates electrode topology, enabling more effective modeling of spatial relationships compared to conventional approaches that depend heavily on channel density.

Despite these advantages, when applied independently, both methods still have limitations. SWT operates on a per-channel basis and does not account for spatial dependencies, leaving inter-channel noise unresolved [6], [18]. Conversely, SPHARA focuses on spatially correlated noise but does not address temporal artifacts occurring within individual channels [7]. Therefore, neither method alone is sufficient to achieve comprehensive EEG denoising.

To address these limitations, this study proposes an integrated preprocessing framework that combines temporal denoising using SWT and spatial filtering using SPHARA for low-density EEG recordings. This approach is designed to simultaneously reduce temporal disturbances and spatial noise while maintaining compatibility with 16-channel EEG systems commonly used in ASD studies.

More importantly, the proposed integration is not a simple combination of two independent methods but a structured dual-domain framework. SWT is first applied to stabilize the signal at the channel level by suppressing transient and non-stationary artifacts. This step is critical, as strong temporal disturbances may propagate across channels and interfere with spatial filtering. Once the signal is temporally refined, SPHARA is applied to model spatial relationships more accurately and suppress correlated noise across channels. This sequential interaction creates a synergistic effect, where temporal stabilization enhances the effectiveness of spatial filtering, resulting in improved overall signal quality.

### 3. Proposed Method

This study aims to develop an EEG preprocessing method for individuals with ASD by integrating temporal and spatial processing stages within a 15-minute recording. The preprocessing pipeline begins with per-channel processing, including basic filtering using FIR (0.5–70 Hz), a 50 Hz notch filter, and detrending, followed by temporal denoising using SWT with the Daubechies 4 (db4) wavelet. The process is then extended to multichannel processing using SPHARA for spatial filtering. The performance of the proposed method is evaluated on a within-subject basis through both visual inspection and quantitative metrics (SNR, MAE, RMSE, and SD) across four pipeline configurations, ranging from FIR-only preprocessing to the full integration of FIR, SWT, and SPHARA. The overall preprocessing pipeline proposed in this study is illustrated in Figure 1. The pipeline consists of dataset acquisition (16-channel EEG, 250 Hz), preprocessing stages (FIR filtering followed by SWT, SPHARA, or their combination), and performance evaluation using SNR, MAE, RMSE, and SD.

#### 3.1. Material

The dataset used in this study consists of EEG signals acquired in raw format from participants using the OpenBCI Cyton Board. This dataset is the same as that reported in a previous study [9] and includes ten participants in Banda Aceh, Indonesia, divided into two groups. The first group consists of five adolescents and young adults aged 15–25 years diagnosed with ASD, recruited from local special schools. The second group consists of five neurotypical individuals aged 17–25 years from the Syiah Kuala University area. Although the dataset includes both ASD and neurotypical subjects, this study focuses specifically on the ASD group to evaluate the effectiveness of the proposed preprocessing pipeline on EEG signals associated with ASD.

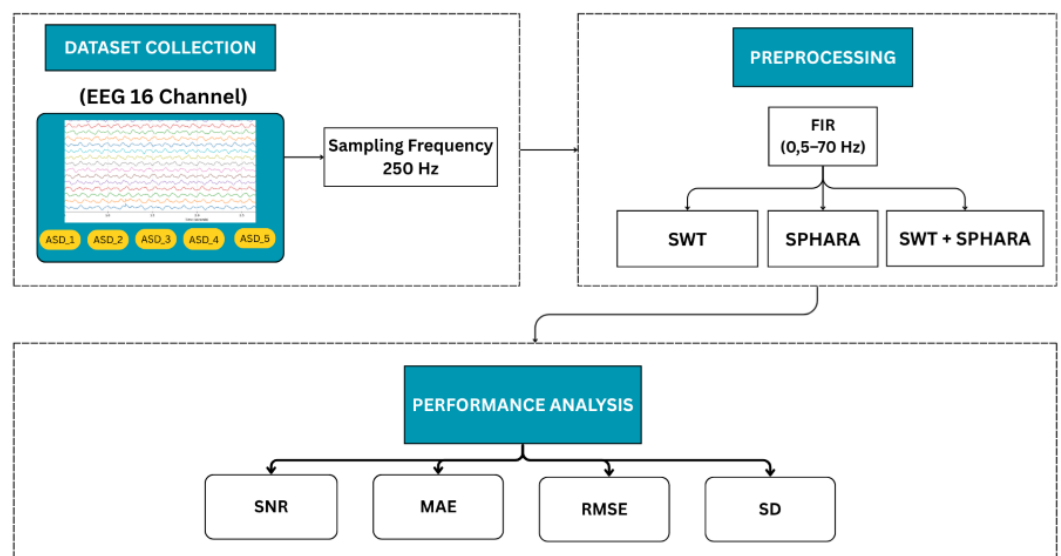


Figure 1. Block diagram of the proposed EEG preprocessing framework.

Data collection was conducted in a quiet and controlled environment between 09:00 and 12:00 [19] to maintain stable participant conditions. Each recording session lasted approximately 40 minutes, including about 10 minutes for electrode preparation and installation, followed by two resting-state recording sessions of 15 minutes each. EEG signals were recorded using a 16-channel configuration based on the international 10–20 electrode placement system, with a sampling frequency of 250 Hz. All research procedures were approved by the Ethics Committee (Reference No. 117/EA/FK/2024) and conducted in accordance with WHO 2011 standards [20].

A reference electrode and a ground electrode were applied during data acquisition using the OpenBCI Cyton Board to ensure signal stability. Participants were instructed to remain relaxed and minimize movement during the recording session to reduce motion-related artifacts. The recorded EEG data were stored in raw format and organized per subject and session. Each recording consists of multichannel time-series data sampled at 250 Hz, which are then processed through the proposed preprocessing pipeline.

### 3.2. Finite Impulse Response (FIR)

FIR is a stable digital filter with a finite impulse response, widely used in EEG signal processing due to its ability to maintain phase linearity, ensuring that the original signal waveform is not distorted [21]. This linear-phase characteristic is achieved by symmetrically arranging the filter coefficients, satisfying the condition  $b[k] = b[M - k]$  where  $M$  is the filter order and  $k$  is the coefficient index. Mathematically, the filter output is generated through a finite convolution process as shown in Equation (1) [21]:

$$y[n] = \sum_{k=0}^M b[k]x[n - k] \quad (1)$$

where  $y[n]$  is the output signal,  $x[n]$  is an input signal, and  $b[k]$  is the filter coefficient. In its implementation as a band-pass filter (0.5–70 Hz), the filter coefficient is formed by limiting the ideal impulse response  $h_d[k]$  Using the window function  $w[k]$  through equations  $b[k] = h_d[k] \cdot w[k]$ . The frequency response of the filter is given in Equation (2) [22]:

$$H(e^{j\omega}) = \sum_{k=0}^M b[k]e^{-j\omega k} \quad (2)$$

with  $H(e^{j\omega})$  in response to frequency,  $\omega$  as angular frequencies, and as imaginary units, which allow filters to maintain the physiological frequency of the EEG while precisely suppressing noise.

The FIR band-pass filter was designed with an order of 800 (801 taps) to ensure an optimal balance between frequency selectivity and computational efficiency. The cutoff frequencies were set to 0.5–70 Hz based on standard EEG preprocessing practices.

### 3.3. Stationary Wavelet Transform (SWT)

SWT is applied as a temporal denoising method due to its translation-invariant property, where no down-sampling is performed, ensuring that the coefficient length remains equal to the original signal length and preserving the peak positions of EEG waveforms. The signal decomposition process  $x[n]$  at each level  $j$  is carried out using an upsampled filter, resulting in an approximation coefficient  $a_{j+1}[n]$  and details  $d_{j+1}[n]$  as shown in Equation (3) [18]:

$$a_{j+1}[n] = \sum_k h_j[k]a_j[n - k], \quad d_{j+1}[n] = \sum_k g_j[k]a_j[n - k] \quad (3)$$

where  $h_j$  and  $g_j$  successively are the low-pass and high-pass filters. To reduce noise, an estimated noise level is carried out  $\hat{\sigma}$  using the Median Absolute Deviation (MAD) of the first-level detail coefficient ( $D_1$ ) with formula  $\hat{\sigma} = \text{median}(|D_1 - \text{median}(D_1)|)/0.674$ . This value is used to determine the universal threshold  $\lambda$  as shown in Equation (4):

$$\lambda = \hat{\sigma}\sqrt{2 \ln N} \quad (4)$$

with  $N$  as sample quantity. Threshold  $\lambda$  It is then applied using the soft thresholding function as given in Equation (5) :

$$\eta_{\text{soft}}(w, \lambda) = \text{sgn}(w) \cdot \max(|w| - \lambda, 0) \quad (5)$$

where  $w$  is the input coefficient and SGN is the signum function, which results in a smoother reconstruction signal by minimizing the noise component without damaging the main signal structure [18].

For temporal denoising, the SWT was implemented using the db4 wavelet with a decomposition level of 6, which was chosen to effectively capture EEG frequency components while preserving signal characteristics.

### 3.4. SPHERICAL HARMONIC ANALYSIS (SPHARA)

SPHARA is a spatial filtering method that utilizes the geometry of the electrode configuration to separate structured global signals from local noise using harmonic bases derived from the eigendecomposition of the discrete Laplace–Beltrami operator. This eigenequation is expressed in Equation (6) [7]:

$$Lx_i = \lambda_i x_i \quad (6)$$

where  $L$  is a Laplacian matrix that represents the topology of the electrode,  $x_i$  is a spatial-based vector, and  $\lambda_i$  is an eigenvalue or spatial frequency. The instantaneous EEG signals ( $f$ ). It is then transformed into a harmonic domain to obtain the contribution coefficient ( $c$ ) as shown in Equation (7) [23]:

$$c^T = f^T X \quad (7)$$

with  $X$  as a base matrix of SPHARA. For the clarification process, a low-order base selection was carried out using a diagonal selection matrix  $R$  to form a spatial filter  $F$ . This filter is then applied to the raw multichannel data ( $D$ ) to generate a clean signal ( $\tilde{D}$ ) as given in Eq. (8):

$$F = RX(RX)^T, \quad \tilde{D} = DF \quad (8)$$

This process effectively suppresses high-frequency spatial noise (e.g., sensor noise) while preserving the temporal integrity of the EEG signal.

In this study, low-order spatial harmonics are retained to preserve dominant spatial patterns, while higher-order components associated with noise are suppressed. This approach enables effective reduction of spatially correlated noise while preserving the essential characteristics of EEG signals [7].

### 3.5. Evaluation Metrics

#### 3.5.1 Signal-to-Noise Ratio (SNR)

SNR is a standard evaluation metric used to measure signal quality by comparing the amount of information signal energy to noise energy in decibels (dB) [24]. In the context of EEG processing, high SNR values indicate that the signal is getting cleaner and free of artifacts, which is crucial for the accuracy of clinical analysis. Quantitatively, SNR is calculated based on a logarithmic comparison between the energy of the reference signal (ground-truth) and the energy of the estimated difference (noise) as shown in Equation (9) [25]:

$$SNR = 10 \log_{10} \left( \frac{\sum_{n=1}^N x[n]^2}{\sum_{n=1}^N (x[n] - \hat{x}[n])^2} \right) \quad (9)$$

where  $x[n]$  Represents a reference signal,  $\hat{x}[n]$  is a signal of estimation or preprocessing, and  $N$  is the total number of samples. This formula shows that the smaller the difference between the original signal and the processing result (the smaller the denominator), the greater the SNR value.

#### 3.5.2 Mean Absolute Error (MAE)

MAE is an evaluation metric used to measure the average amount of error between the processing signal (prediction) and the reference signal, regardless of the direction of the

positive or negative deviation [26]. This metric provides a direct picture of how close the reconstruction results are to the original data, where smaller values indicate better and more accurate model performance. Mathematically, MAE is calculated by flattening the absolute difference of each sample point as shown in Equation (10) [27]:

$$MAE = \frac{1}{N} \sum_{i=1}^N |x_i - y_i| \quad (10)$$

where  $x_i$  is the actual signal value (reference),  $y_i$  is the value of the prediction signal or processing result, and  $N$  is the total number of observation samples.

### 3.5.3 Root Mean Square Error (RMSE)

RMSE is a square-based evaluation metric used to measure the magnitude of the deviation between the predicted signal and the reference signal, with the main characteristic that provides a greater penalty for extreme amplitude errors compared to MAE [28]. Because the final result has the same unit as the original data, the RMSE facilitates the interpretation of the typical magnitude of the error in EEG signal reconstruction, where the smaller values signal a low mean deviation and better model performance. Mathematically, RMSE is calculated through the root operation of the mean of the square of the difference as shown in Equation (11) [29]:

$$RMSE = \sqrt{\frac{1}{N} \sum_{n=1}^N (x[n] - \hat{x}[n])^2} \quad (11)$$

where  $x[n]$  is the actual signal value (reference),  $\hat{x}[n]$  is the value of the prediction signal, and  $N$  is the total number of observation samples.

### 3.5.4 Standard Deviation (SD)

SD is a statistical measure that represents the level of dispersion or dispersion of data relative to its mean value. By definition, SD is the square root of variance, where a high value indicates that the data is widely dispersed from its center, while a low value indicates that the data tends to cluster around the mean value [30]. This metric is crucial to determine how far observation values deviate from their expected values. Mathematically, for a sample of data, the standard deviation is calculated as shown in Eq. (12) :

$$s = \sqrt{\frac{\sum_{i=1}^n (x_i - \bar{x})^2}{n - 1}} \quad (12)$$

where  $s$  is the standard deviation,  $x_i$  is the observation value to- $i$ ,  $\bar{x}$  is the average value of the sample, and  $n$  is the size or number of samples.

## 4. Results and Discussion

The results obtained from EEG signal processing are presented as follows. First, the signals are processed using a basic filtering stage consisting of FIR band-pass filtering (0.5–70 Hz), a 50 Hz notch filter, and detrending. The output of this stage is then used as input for temporal denoising using SWT with the db4 wavelet. The resulting signals are subsequently processed in a multichannel framework using SPHARA for spatial filtering. The final output of the pipeline is a signal that has been refined both temporally and spatially. The performance of the reconstructed signals is evaluated using four quantitative metrics: SNR, MAE, RMSE, and SD. The qualitative comparison of EEG signals at each preprocessing stage is shown in Figure 2. The figure illustrates the progressive reduction of noise and improvement of signal stability across preprocessing stages.

### 4.1. FIR Filter Results

The initial preprocessing stage using FIR band-pass filtering (0.5–70 Hz), combined with a 50 Hz notch filter and detrending, effectively suppresses non-essential frequency components and electrical interference. A significant baseline correction is observed, where DC offsets that initially reach tens of thousands of  $\mu\text{V}$  in raw signals are reduced to the order of

hundreds of  $\mu\text{V}$ . However, the FIR-filtered signals still exhibit high temporal variability. For example, the SD ( $\sigma$ ) in certain channels, such as F4, remains in the range of approximately 3000  $\mu\text{V}$  (Fig. 2). This indicates that non-stationary artifacts and channel-specific noise are not fully addressed by linear filtering alone. Such artifacts, including eye blinks, muscle activity, and electrode movement, typically manifest as transient fluctuations and require more adaptive denoising approaches.

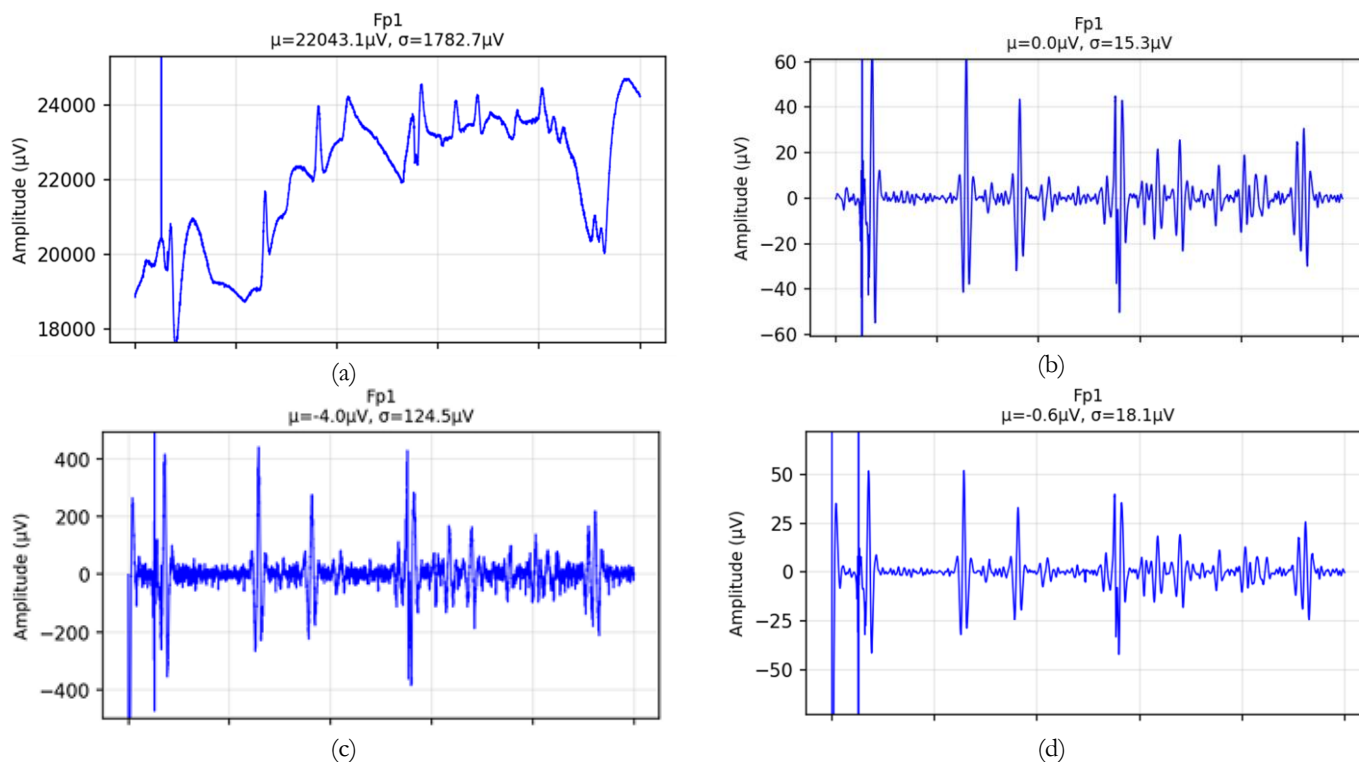


**Figure 2.** Representative EEG signals (Fp1 channel) at different preprocessing stages: (a) FIR filtering; (b) FIR + SWT; (c) FIR + SPHARA; and (d) FIR + SWT + SPHARA.

#### 4.2. Denoising Results with SWT

The application of SWT (db4) to FIR-filtered signals results in clear qualitative and quantitative improvements. The mean value ( $\mu$ ) across channels becomes closer to zero (e.g., 0.1–17.3  $\mu\text{V}$ ), indicating improved baseline stabilization. More importantly, the SD ( $\sigma$ ) is significantly reduced; for instance, in channel F4,  $\sigma$  decreases to 432.8  $\mu\text{V}$  (Figure 2).

These results demonstrate the effectiveness of SWT in suppressing non-linear and non-stationary temporal artifacts that are not adequately removed by linear filtering. Unlike conventional filtering methods, SWT preserves the temporal structure of the signal while decomposing it across multiple frequency scales. This enables more effective separation of transient artifacts from the underlying neural activity.

#### 4.3. Spatial Filtering Results with SPHARA

Spatial filtering using SPHARA applied to FIR-filtered signals shows the ability to reduce spatially correlated noise across channels. The mean value ( $\mu$ ) remains close to zero; however, the SD ( $\sigma$ ) remains relatively high. For example, in channel F4,  $\sigma$  is recorded at 2997.9  $\mu\text{V}$  (Figure 2), indicating that substantial variability persists.

This suggests that spatial filtering alone is insufficient to address artifacts that originate locally within individual channels. While SPHARA is effective in suppressing global, inter-channel noise, it does not adequately handle independent temporal artifacts at the electrode level. These findings highlight the necessity of incorporating a temporal denoising stage prior to spatial filtering.

#### 4.4 Results of the Integrated FIR–SWT–SPHARA Pipeline

The integration of FIR, SWT, and SPHARA yields the most effective preprocessing performance among all configurations. The output signals from the combined pipeline exhibit the most stable characteristics, with mean values ( $\mu$ ) close to zero (e.g.,  $-3.0$  to  $16.3 \mu\text{V}$ ) and the lowest SD ( $\sigma$ ). In channel F4,  $\sigma$  is reduced to  $412.6 \mu\text{V}$  (Fig. 2).

These results indicate a clear synergy between temporal and spatial preprocessing. SWT first stabilizes the signal at the channel level by removing transient artifacts, thereby providing a cleaner input for SPHARA. Subsequently, SPHARA more effectively reduces spatially correlated noise across channels. This sequential interaction enhances the overall denoising performance.

Overall, the integrated pipeline produces EEG signals with improved stability and reduced noise, demonstrating that temporal and spatial preprocessing methods provide complementary advantages. Temporal denoising addresses local, non-stationary artifacts, while spatial filtering reduces global noise across channels, resulting in a more reliable signal representation for further analysis.

#### 4.5 Method Performance Evaluation

##### 4.5.1. Signal-to-Noise Ratio Analysis

The SNR results clearly show that the FIR–SWT–SPHARA pipeline consistently achieves the highest values across all ASD subjects (Figure 3).

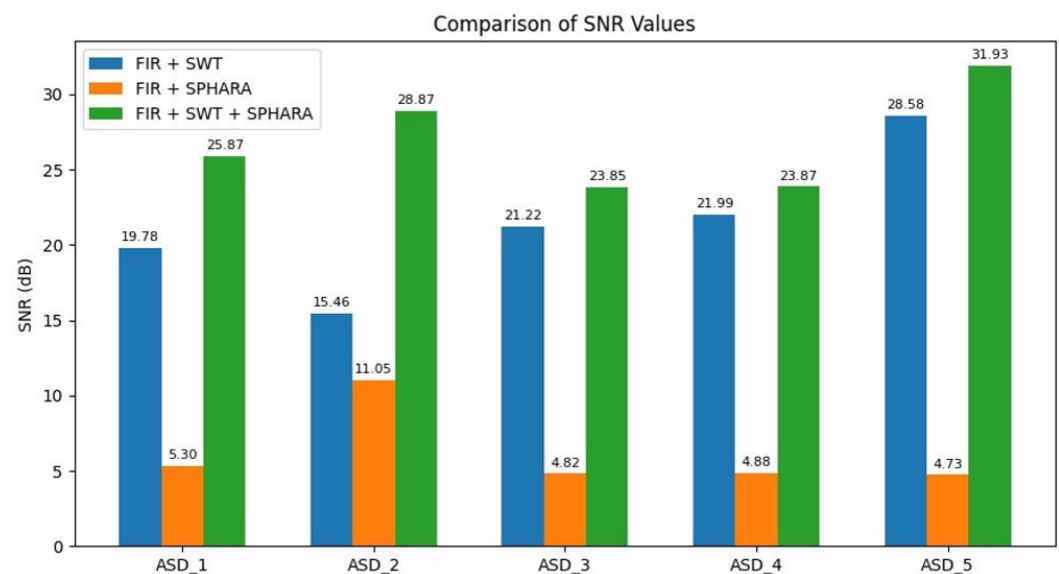


**Figure 3.** Comparison of SNR values across ASD subjects for different preprocessing methods. The FIR–SWT–SPHARA pipeline consistently achieves the highest SNR, indicating improved signal-to-noise separation.

The improvement is not marginal but substantial, particularly when compared to FIR + SPHARA, which produces significantly lower SNR values in all cases. This pattern highlights an important observation: temporal denoising plays a critical role in improving signal clarity. FIR + SWT already produces a notable increase in SNR, but the addition of SPHARA further enhances performance, indicating that spatial filtering becomes more effective once temporal artifacts have been suppressed. The highest SNR is observed in ASD\_5 (31.93 dB), suggesting that the combined pipeline is particularly effective in scenarios where both temporal and spatial noise components are present. Overall, these results demonstrate that the integration of SWT and SPHARA provides a complementary mechanism for improving signal quality, where temporal stabilization enables more effective spatial noise reduction.

#### 4.5.2. Mean Absolute Error Analysis

The MAE results reveal a more nuanced behavior compared to SNR (Figure 4). While the FIR–SWT–SPHARA pipeline generally produces low and stable MAE values, it does not consistently achieve the lowest error across all subjects. In several cases (e.g., ASD\_2 and ASD\_3), FIR + SWT produces slightly lower MAE values than the integrated pipeline. This indicates that temporal denoising alone is highly effective in preserving the original signal structure, while the addition of spatial filtering may introduce minor deviations.

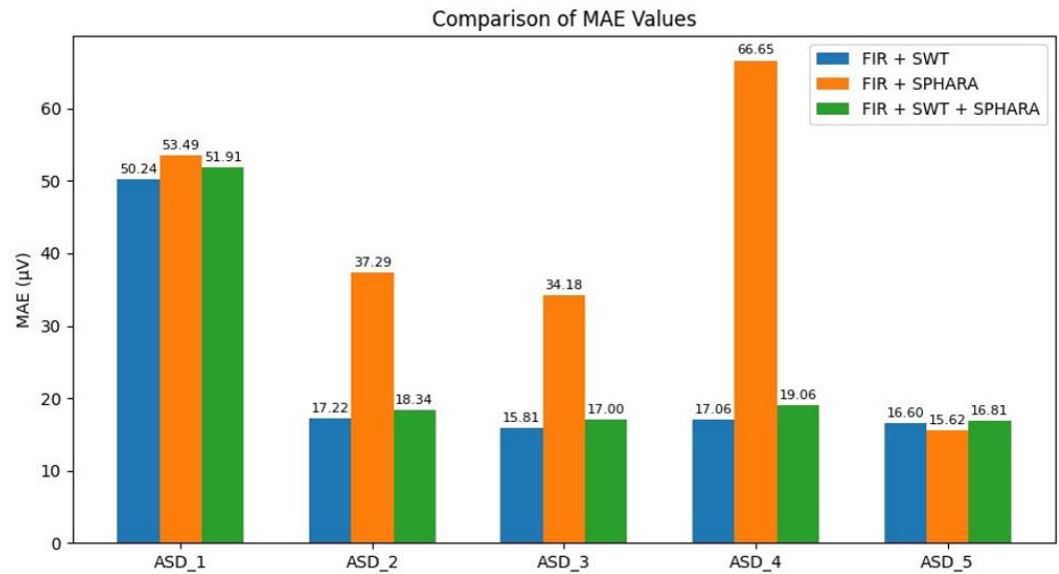


Figure 4. Comparison of MAE values across ASD subjects.

However, a key observation emerges in ASD\_4, where FIR + SPHARA produces a significantly higher MAE (66.65  $\mu\text{V}$ ), while the integrated pipeline reduces it drastically to 19.06  $\mu\text{V}$ . This demonstrates that the combination approach is more robust in handling complex noise conditions, even if it does not always minimize point-wise error. These findings suggest a trade-off:

- FIR + SWT  $\rightarrow$  better signal fidelity (lower MAE)
- FIR–SWT–SPHARA  $\rightarrow$  better overall robustness

Thus, the proposed pipeline maintains a good balance between noise suppression and structural preservation.

#### 4.5.3. Standard Deviation Analysis

The SD results provide the most consistent evidence of the effectiveness of the proposed method (Figure 5). Across all ASD subjects, the FIR–SWT–SPHARA pipeline produces the lowest SD values, indicating significantly reduced amplitude variability. This result is particularly important because SD reflects signal stability rather than point-wise accuracy. The drastic reduction in SD—from values exceeding 200  $\mu\text{V}$  (FIR + SPHARA) to below 25  $\mu\text{V}$  in most cases—indicates that noise-induced fluctuations have been effectively suppressed.

Unlike MAE and RMSE, which depend on a reference signal, SD directly reflects the internal consistency of the processed signal. Therefore, the consistently low SD values strongly support the conclusion that the integrated pipeline produces more stable and reliable EEG signals. This also reinforces the complementary roles of SWT and SPHARA:

- SWT reduces local, transient fluctuations
  - SPHARA suppresses global, spatially correlated noise
- Together, they produce a signal with significantly improved stability.

#### 4.5.4. Root Mean Square Error Analysis

The RMSE results show that the FIR–SWT–SPHARA pipeline achieves moderate but stable performance across all subjects (Figure 6). Unlike SNR and SD, the integrated method does not consistently yield the lowest RMSE values. This observation is important and should be interpreted carefully. RMSE measures the overall energy difference between the processed

signal and the reference signal. Since the reference signal is not a true noise-free ground truth, lower RMSE does not necessarily indicate better denoising performance. For example, FIR + SPHARA often produces lower RMSE values, but this does not correspond to better signal quality when considering SNR and SD. This suggests that RMSE alone is insufficient to evaluate denoising performance in real EEG data.

The integrated pipeline maintains RMSE within a stable range while significantly improving SNR and SD. This indicates that the method effectively reduces noise without excessively distorting the signal structure. Overall, the RMSE results highlight an important trade-off between signal fidelity and noise suppression, where the proposed method prioritizes stability and clarity over minimal deviation from the reference signal.

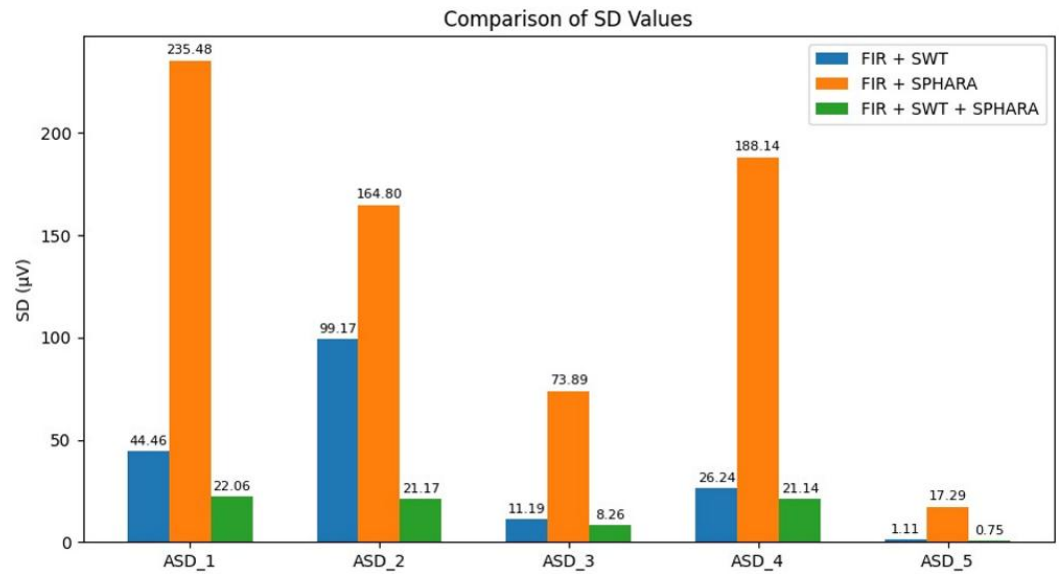


Figure 5. Comparison of SD values across ASD subjects.

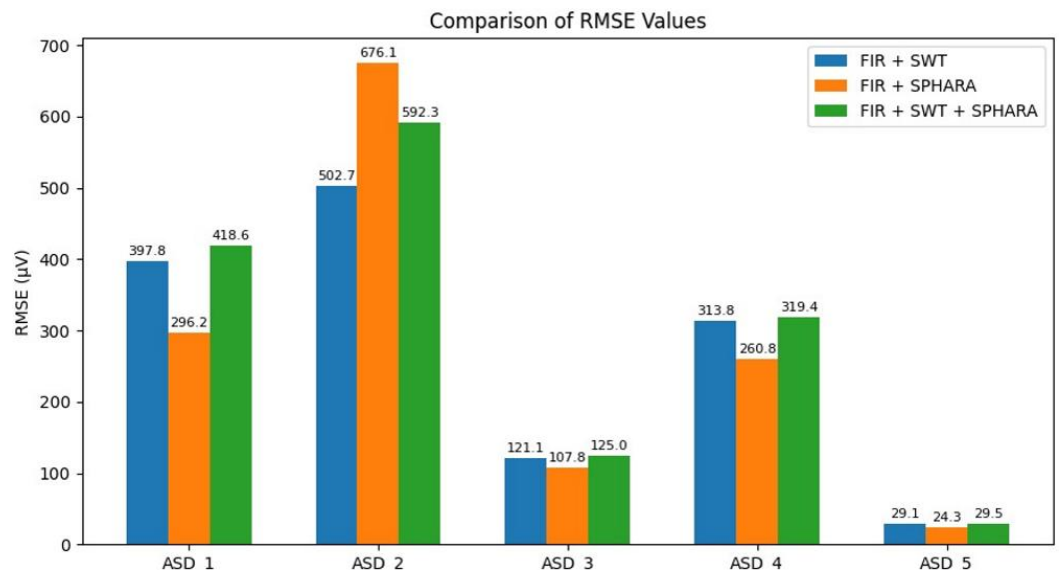


Figure 6. Comparison of RMSE values across ASD subjects.

### 5. Discussion

The results demonstrate that integrating temporal and spatial preprocessing provides superior EEG signal quality compared to single-method approaches. The FIR-SWT-SPHARA pipeline consistently achieves the highest SNR across all ASD subjects, with a maximum value of 31.93 dB, exceeding both temporal-only methods (15.46–28.58 dB) and spatial-only approaches (generally below 11.05 dB). This confirms that EEG artifacts inherently

exhibit both temporal and spatial characteristics, and therefore require a combined processing strategy.

In addition to the improvement in SNR, the integrated approach produces low MAE and the lowest SD, indicating reduced amplitude distortion and improved signal stability. Among the evaluated metrics, SD provides the most consistent improvement across subjects, reflecting effective suppression of noise-induced fluctuations. In contrast, RMSE values remain within a comparable range across methods, suggesting that the proposed pipeline preserves overall signal energy while reducing noise.

These results highlight an important distinction between evaluation metrics. While MAE and RMSE measure deviation from a reference signal, SD reflects intrinsic signal stability. Therefore, the consistently low SD values provide stronger evidence that the proposed method produces stable and reliable EEG signals, even when improvements in MAE and RMSE are not always dominant. It is important to note that the original EEG signal is used as the reference for computing MAE, RMSE, and SNR. However, this signal is not a true ground truth, as it contains inherent noise and artifacts. Consequently, these metrics provide relative comparisons rather than absolute measures of signal accuracy, and their interpretation should be made with caution. To address this limitation, a reference-free evaluation based on relative band power is conducted, as shown in Figure 7.

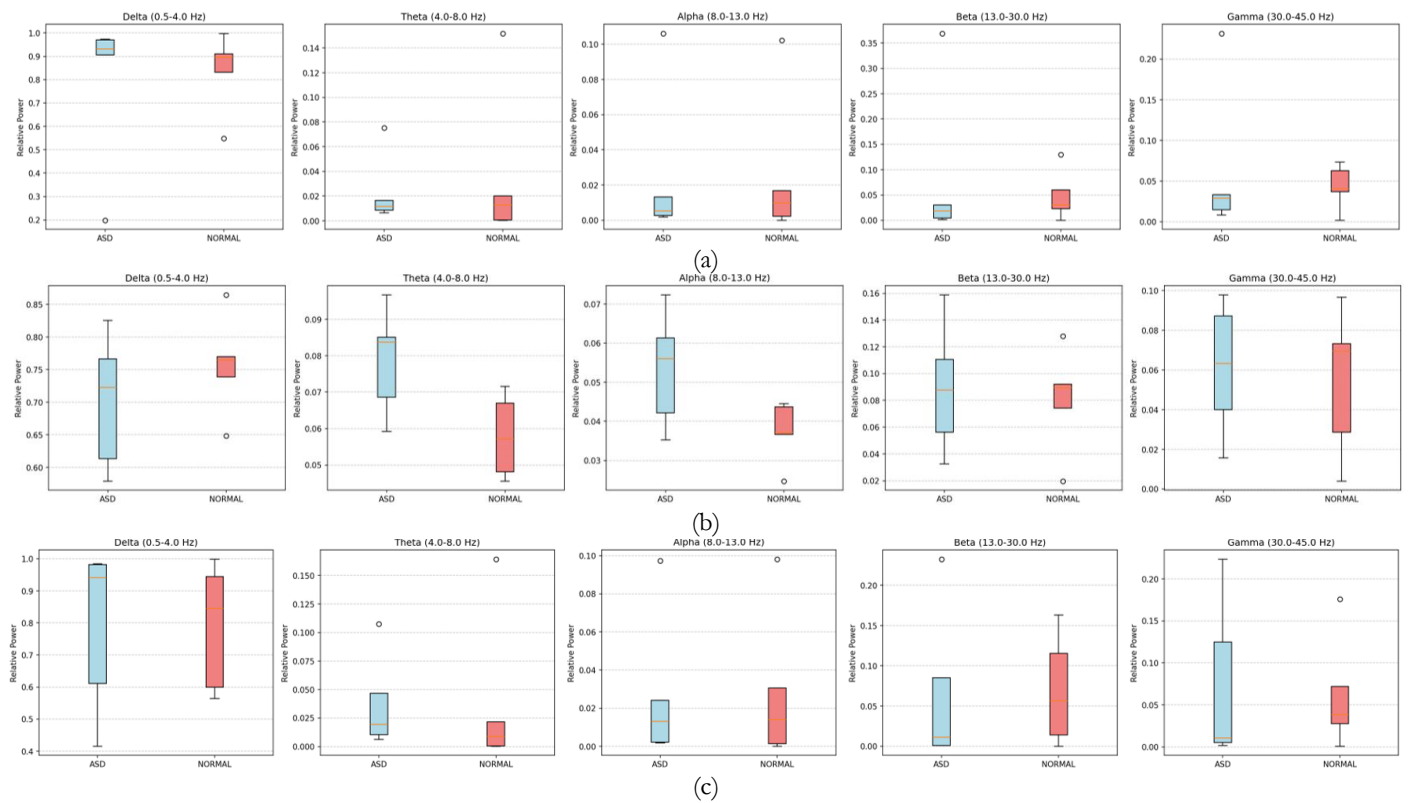


**Figure 7.** Relative band power comparison (delta, theta, alpha, beta, and gamma bands) across preprocessing methods: (a) FIR + SWT, (b) FIR + SPHARA, and (c) FIR-SWT-SPHARA.

The band power analysis shows that the integrated method produces a more consistent spectral distribution across subjects, particularly in higher-frequency bands (beta and gamma), which are typically more sensitive to noise. This indicates that the proposed pipeline effectively suppresses noise while preserving physiologically meaningful EEG components. Unlike MAE and RMSE, band power reflects intrinsic signal characteristics and is therefore more suitable for evaluating real-world EEG data.

To further validate the effectiveness of the proposed method, comparisons with previous studies were considered. For example, EEG preprocessing using a Butterworth band-pass filter achieved a maximum SNR of only 1.33 dB, indicating limited noise suppression capability [31]. More advanced temporal approaches, such as Multiscale Independent Component Analysis (MS-ICA), improved SNR to the range of 21.77–30.88 dB [31]. Similarly,

combining Butterworth filtering with EMD achieved a maximum SNR of 23.208 dB [32]. In contrast, the proposed method achieves a higher maximum SNR of 31.93 dB, suggesting that integrating temporal and spatial processing can further enhance EEG signal quality beyond temporal-only approaches. It should be noted, however, that direct comparisons across studies may be influenced by differences in datasets, experimental settings, and evaluation metrics.

Aggregate analysis across all ASD subjects further supports these findings. The proposed method achieves the highest average SNR ( $26.88 \pm 3.12$  dB) and the lowest SD ( $14.68 \pm 8.64$   $\mu$ V), indicating improved signal clarity and stability compared to FIR + SWT ( $21.41 \pm 4.24$  dB;  $36.43 \pm 34.60$   $\mu$ V) and FIR + SPHARA ( $6.16 \pm 2.46$  dB;  $135.92 \pm 79.20$   $\mu$ V). Meanwhile, MAE ( $24.62 \pm 13.67$   $\mu$ V) remains comparable to FIR + SWT ( $23.39 \pm 13.43$   $\mu$ V), and RMSE ( $296.96 \pm 201.80$   $\mu$ V) remains within a similar range across methods. These results indicate that the proposed approach improves noise suppression without significantly compromising signal structure.

The effectiveness of the pipeline is closely related to the selected processing order. FIR filtering is first applied to remove baseline drift and frequency-specific noise. SWT then performs temporal denoising at the channel level, stabilizing the signal by suppressing transient artifacts. Finally, SPHARA is applied to remove spatially correlated noise after temporal disturbances have been minimized. This sequential design ensures that spatial filtering operates on a temporally stabilized signal, thereby avoiding misinterpretation of transient artifacts as spatial patterns. In contrast, reversing this order may lead to suboptimal results, as spatial filtering would be applied to signals that still contain significant temporal noise.

Compared to existing approaches, the proposed method provides a unified framework that simultaneously addresses temporal and spatial noise. While many previous methods focus on either temporal decomposition (e.g., EMD) or spatial filtering (e.g., ICA), the integration of SWT and SPHARA enables more comprehensive noise suppression. Moreover, the method is specifically designed for low-density EEG configurations, making it more practical for real-world applications.

Despite these advantages, the proposed method does not always achieve the lowest MAE and RMSE values. This reflects a trade-off between noise suppression and signal fidelity. While the method prioritizes cleaner and more stable signals, minor deviations from the original signal may occur. Such a trade-off is acceptable in applications where signal clarity and robustness are more critical than exact reconstruction. Finally, it should be noted that the evaluation is conducted on a relatively small internal dataset focusing on ASD subjects, which may limit generalizability. Future work may include evaluation on larger and publicly available datasets, as well as integration with machine learning or deep learning models for EEG-based classification tasks..

## 6. Conclusions

This study proposes an EEG preprocessing pipeline that integrates temporal and spatial processing using FIR band-pass filtering, SWT, and SPHARA to improve EEG signal quality in individuals with ASD. The results demonstrate that the integrated approach consistently provides superior performance compared to single-method preprocessing techniques. The observed improvement in SNR indicates that the proposed method effectively suppresses both temporal and spatial noise components. At the same time, the relatively low MAE and stable RMSE values suggest that the method preserves essential signal characteristics while reducing noise. In addition, the low SD reflects improved signal stability and reduced variability.

These findings indicate that the proposed method achieves a balance between noise suppression and signal preservation. This balance is critical in EEG preprocessing, as excessive denoising may distort meaningful neural information, whereas insufficient noise removal may reduce signal reliability. Overall, the FIR–SWT–SPHARA framework produces cleaner, more stable, and more representative EEG signals, making it suitable for subsequent analysis, particularly in low-density EEG systems.

Despite these advantages, several limitations should be noted. The evaluation was conducted on a relatively small internal dataset focusing only on ASD subjects, which may limit generalizability. In addition, the evaluation primarily relies on signal quality metrics without validation on larger or publicly available datasets. Furthermore, the performance of the proposed pipeline may depend on parameter selection, including the FIR filter design, the SWT

decomposition level, and the number of spatial harmonics used in SPHARA. These parameters were determined empirically in this study, and further investigation is required to analyze their sensitivity and optimize their configuration across different EEG datasets. Future work will focus on evaluating the proposed framework on larger and publicly available EEG datasets, as well as integrating it with machine learning and deep learning models for automated ASD classification. In addition, extending this approach to real-time EEG systems may provide further insights for clinical applications..

**Author Contributions:** Conceptualization: C.S.A.S. and M.M.; Methodology: C.S.A.S. and S.S.; Software: C.S.A.S.; Validation: M.M., S.S., S.D., and M.A.H.; Formal analysis: C.S.A.S.; Investigation: C.S.A.S.; Resources: M.M.; Data curation: I.F.R.; Writing—original draft preparation: C.S.A.S. and I.F.R.; Writing—review and editing: M.M., S.D., and M.A.H.; Visualization: I.F.R.; Supervision: M.M.; Project administration: M.M. All authors have read and agreed to the published version of the manuscript.

**Funding:** This research received no external funding.

**Data Availability Statement:** Data are contained within the article.

**Acknowledgments:** The author expresses heartfelt gratitude to Syiah Kuala University for its assistance with this study. This assistance encompassed a learning environment that promoted ongoing development in addition to facilities and resources. Additionally, the author is grateful for the direction and inspiration provided by faculty members. Without the institution's sincere dedication to fostering scientific research in medical electronic technology, this study would not have progressed to its ultimate phase.

**Conflicts of Interest:** The authors declare no conflict of interest

## References

- [1] J. Zeidan *et al.*, “Global prevalence of autism: A systematic review update,” *Autism Res.*, vol. 15, no. 5, pp. 778–790, May 2022, doi: 10.1002/aur.2696.
- [2] I. Kamp-Becker *et al.*, “Is the Combination of ADOS and ADI-R Necessary to Classify ASD? Rethinking the ‘Gold Standard’ in Diagnosing ASD,” *Front. Psychiatry*, vol. 12, Aug. 2021, doi: 10.3389/fpsyt.2021.727308.
- [3] P. Wantzen *et al.*, “EEG resting-state functional connectivity: evidence for an imbalance of external/internal information integration in autism,” *J. Neurodev. Disord.*, vol. 14, no. 1, p. 47, Dec. 2022, doi: 10.1186/s11689-022-09456-8.
- [4] P. Garcés *et al.*, “Resting state EEG power spectrum and functional connectivity in autism: a cross-sectional analysis,” *Mol. Autism*, vol. 13, no. 1, p. 22, Dec. 2022, doi: 10.1186/s13229-022-00500-x.
- [5] R. Kessler, A. Engé, and M. A. Skeide, “How EEG preprocessing shapes decoding performance,” *Commun. Biol.*, vol. 8, no. 1, p. 1039, Jul. 2025, doi: 10.1038/s42003-025-08464-3.
- [6] M. C. Piastra, R. Oostenveld, S. Homölle, B. Han, Q. Chen, and T. Oostendorp, “How to assess the accuracy of volume conduction models? A validation study with stereotactic EEG data,” *Front. Hum. Neurosci.*, vol. 18, Feb. 2024, doi: 10.3389/fnhum.2024.1279183.
- [7] M. Komosar, G. Tamburro, U. Graichen, S. Comani, and J. Hauelsen, “Combination of spatial and temporal de-noising and artifact reduction techniques in multi-channel dry EEG,” *Front. Neurosci.*, vol. 19, Jun. 2025, doi: 10.3389/fnins.2025.1576954.
- [8] A. Asayesh, S. Vanhatalo, and A. Tokariev, “The impact of EEG electrode density on the mapping of cortical activity networks in infants,” *Neuroimage*, vol. 303, p. 120932, Dec. 2024, doi: 10.1016/j.neuroimage.2024.120932.
- [9] M. Melinda *et al.*, “Feature-Based EEG Classification: A Comparative Study of EMD and EWT With EEGNet and Shallow FBCSP ConvNet,” *IEEE Access*, vol. 13, pp. 185095–185110, 2025, doi: 10.1109/ACCESS.2025.3625234.
- [10] A. Wang and J. Sun, “Personalized EEG-guided brain stimulation targeting in major depression via network controllability and multi-objective optimization,” *BMC Psychiatry*, vol. 25, no. 1, p. 723, Jul. 2025, doi: 10.1186/s12888-025-07171-x.
- [11] T. Hirota and B. H. King, “Autism Spectrum Disorder,” *JAMA*, vol. 329, no. 2, p. 157, Jan. 2023, doi: 10.1001/jama.2022.23661.
- [12] National Institute of Mental Health, “Autism Spectrum Disorder,” 2008. Accessed: Jan. 12, 2026. [Online]. Available: <https://www.nimh.nih.gov/sites/default/files/documents/health/publications/autism-spectrum-disorder/autism-spectrum-disorder.pdf>
- [13] Y. Xu, Z. Yu, Y. Li, Y. Liu, Y. Li, and Y. Wang, “Autism spectrum disorder diagnosis with EEG signals using time series maps of brain functional connectivity and a combined CNN–LSTM model,” *Comput. Methods Programs Biomed.*, vol. 250, p. 108196, Jun. 2024, doi: 10.1016/j.cmpb.2024.108196.
- [14] V. A. Raj, T. Parupudi, V. K. K., A. Thalengala, and S. G. Nayak, “Physiological Artifact Suppression in EEG Signals Using an Efficient Multi-Scale Depth-Wise Separable Convolution and Variational Attention Deep Learning Model for Improved Neurological Health Signal Quality,” *Technologies*, vol. 13, no. 12, p. 578, Dec. 2025, doi: 10.3390/technologies13120578.
- [15] D. Gorjan, K. Gramann, K. De Pauw, and U. Marusic, “Removal of movement-induced EEG artifacts: current state of the art and guidelines,” *J. Neural Eng.*, vol. 19, no. 1, p. 011004, Feb. 2022, doi: 10.1088/1741-2552/ac542c.

- [16] P. Nagy, B. Tóth, I. Winkler, and Á. Boncz, "The effects of spatial leakage correction on the reliability of EEG-based functional connectivity networks," *Hum. Brain Mapp.*, vol. 45, no. 8, Jun. 2024, doi: 10.1002/hbm.26747.
- [17] J. Iivanainen, A. J. Mäkinen, R. Zetter, M. Stenroos, R. J. Ilmoniemi, and L. Parkkonen, "Spatial sampling of MEG and EEG based on generalized spatial-frequency analysis and optimal design," *Neuroimage*, vol. 245, p. 118747, Dec. 2021, doi: 10.1016/j.neuroimage.2021.118747.
- [18] F. Fahmi, M. Melinda, P. D. Purnamasari, E. Elizar, and A. Rafiki, "Recognition of EEG Features in Autism Disorder Using SWT and Fisher Linear Discriminant Analysis," *Diagnostics*, vol. 15, no. 18, p. 2291, Sep. 2025, doi: 10.3390/diagnostics15182291.
- [19] M. Mulyadi, M. Melinda, Y. Away, and S. Gazali, "Comparative Analysis of Normal and ASD EEG Data Using Hjorth Parameters," in *2025 7th International Congress on Human-Computer Interaction, Optimization and Robotic Applications (ICHORA)*, May 2025, pp. 1–6. doi: 10.1109/ICHORA65333.2025.11017066.
- [20] M. Melinda, P. D. Purnamasari, F. Fahmi, E. Sinulingga, M. Mulyadi, and I. A. Yamin, "Innovative Portable Quantitative EEG Data Acquisition Based Cyton Biosensing Board using PSD Analysis," in *2024 10th International Conference on Smart Computing and Communication (ICSCC)*, Jul. 2024, pp. 631–636. doi: 10.1109/ICSCC62041.2024.10690827.
- [21] L. Jiang, H. Zhang, S. Cheng, H. Lv, and P. Li, "An Overview of FIR Filter Design in Future Multicarrier Communication Systems," *Electronics*, vol. 9, no. 4, p. 599, Mar. 2020, doi: 10.3390/electronics9040599.
- [22] H. Hu, S. Song, and Y. Gong, "General FIR Filter Design with Linear Phase in Passband by Water Cycle Algorithm," *J. Comput. Commun.*, vol. 06, no. 11, pp. 326–331, 2018, doi: 10.4236/jcc.2018.611029.
- [23] U. Graichen, R. Eichardt, and J. Haueisen, "SpharaPy: A Python toolbox for spatial harmonic analysis of non-uniformly sampled data," *SoftwareX*, vol. 10, p. 100289, Jul. 2019, doi: 10.1016/j.softx.2019.100289.
- [24] R. Sharanya, D. Sugumar, S. M. Skaria, J. N. Zacharias, and V. J. R. Rosebell, "ICA based informed source separation for watermarked audio signals," in *2011 3rd International Conference on Electronics Computer Technology*, Apr. 2011, pp. 130–134. doi: 10.1109/ICECTECH.2011.5941872.
- [25] S. I. Alzahrani and M. M. Alsaleh, "The Influence of Smoothing Filtering Methods on the Performance of an EEG-Based Brain-Computer Interface," *IEEE Access*, vol. 11, pp. 60171–60180, 2023, doi: 10.1109/ACCESS.2023.3285660.
- [26] I. H. Shakri, "Time series prediction using machine learning: a case of Bitcoin returns," *Stud. Econ. Financ.*, vol. 39, no. 3, pp. 458–470, Apr. 2022, doi: 10.1108/SEF-06-2021-0217.
- [27] S. Fakharchian, "Designing a forecasting assistant of the Bitcoin price based on deep learning using market sentiment analysis and multiple feature extraction," *Soft Comput.*, vol. 27, no. 24, pp. 18803–18827, Dec. 2023, doi: 10.1007/s00500-023-09028-5.
- [28] T. Chai and R. R. Draxler, "Root mean square error (RMSE) or mean absolute error (MAE)? – Arguments against avoiding RMSE in the literature," *Geosci. Model Dev.*, vol. 7, no. 3, pp. 1247–1250, Jun. 2014, doi: 10.5194/gmd-7-1247-2014.
- [29] D. Chicco, M. J. Warrens, and G. Jurman, "The coefficient of determination R-squared is more informative than SMAPE, MAE, MAPE, MSE and RMSE in regression analysis evaluation," *PeerJ Comput. Sci.*, vol. 7, pp. 1–24, 2021, doi: 10.7717/PEERJ-CS.623.
- [30] H. Adeli, Z. Zhou, and N. Dadmehr, "Analysis of EEG records in an epileptic patient using wavelet transform," *J. Neurosci. Methods*, vol. 123, no. 1, pp. 69–87, Feb. 2003, doi: 10.1016/S0165-0270(02)00340-0.
- [31] M. Mirza Rahmat, Y. Nurdin, M. Melinda, Y. Away, M. Irhamsyah, and W. K. Wong, "Autism EEG Signal Pre-Processing: Performance Evaluation of MS-ICA and Butterworth Filter," *Indones. J. Electron. Electromed. Eng. Med. Informatics*, vol. 7, no. 3, pp. 488–500, Aug. 2025, doi: 10.35882/ijeemi.v7i3.107.
- [32] I. Fathur Rahman *et al.*, "EEG Performance Signal Analysis for Diagnosing Autism Spectrum Disorder using Butterworth and Empirical Mode Decomposition," *J. Electron. Electromed. Eng. Med. Informatics*, vol. 7, no. 3, pp. 925–939, Jul. 2025, doi: 10.35882/ijeemi.v7i3.788.